

Scaled laboratory experiments on the evolution of fluidised avalanches.

J. Koegl^{1,2}, A. Graf¹, L. Rammer², K. Kleemayr¹, M.A. Kern^{1*}, P. Gauer¹, G. Kapeller² and M. Aufleger²

¹Federal Research and Training Centre for Forests, Natural Hazards and Landscapes (BFW), Innsbruck, Austria

²Unit of Hydraulic Engineering (IWB), Department of Infrastructure, University of Innsbruck, Innsbruck, Austria

ABSTRACT. Scaled chute experiments with avalanche-like flows of dry granular matter have proven to be a useful tool for the design of technical avalanche protection measures. However, the characteristics of the generated model avalanches have been restricted to the dense flow state so far.

We use a 8 m long and 1 m wide laboratory chute with variable inclination to generate avalanche-like flows that exhibit typical avalanche features such as a rotational head, fingering of the front and a distinct fluidised suspension layer: by careful choice of model materials and boundary conditions, we have been able to access flow states where air drag plays a significant role.

The model avalanches are characterised in terms of flow height, basal flow velocity and by the 2D velocity field derived from a PIV analysis of high-speed camera recordings of the flow through a transparent side-wall of the chute. Furthermore, we characterise the model flows by dimensionless quantities such as Froude-, Stokes- and Reynolds numbers. The results indicate that the values of some of the dimensionless characteristics of the model avalanches match those of real-scale powder avalanches.

High-speed video recordings of the impact of the model avalanches on a scaled snow net demonstrate that the snow net holds back a significant part of the avalanche mass and that the flow state of the mass penetrating and overrunning the snow net undergoes a transition from super- to subcritical flow behaviour.

KEYWORDS: scaled avalanche experiments, snow net, breaking obstacle.

1 INTRODUCTION

Physical modelling is an important methodology for the design of avalanche protection structures. However, this approach has to deal with the fundamental problem of satisfying the governing scaling laws. In particular, the density ratio of suspended snow particles and ambient air $\Delta\rho/\rho$ that is crucial with respect to the Boussinesq-approximation, has to be carefully considered when attempting to model avalanches including their suspended layer (Turnbull and McElwaine, 2008). The large deviations of $\Delta\rho/\rho$ from the real-scale values encountered in water tank experiments

(Hermann and Hutter, 1986; Scheiwiler and Hutter, 1982) suggest that scaled experiments with air as ambient medium (Turnbull and McElwaine, 2008) are a promising alternative.

However, scaled experiments with air as ambient medium have to deal with the problem of choice of appropriate model material (Turnbull and McElwaine, 2008). We present scaled experiments on a laboratory chute that, by careful choice of model materials successfully could reproduce typical mixed dense/powder avalanche features such as front instabilities (fingering), evolution of a suspended flow layer and rotational flow (McElwaine, 2005) at the front. We present model avalanches of various model materials on different chute geometries and characterise them by dimensionless numbers (Stokes, Froude, density ratio), by their velocity profiles close to the front and by their velocity evolution along the chute. Finally, we report

* Corresponding author's address:
Martin Kern
BFW Hofburg - Rennweg 1
6020 Innsbruck, Austria
Tel: ++43 512 573933 5103; Fax: ++43 512 573933 5250;
E-mail: martin.kern@uibk.ac.at

the influence of a permeable obstacle (net structure) called “snowcatcher” that dissipates about 2/3 of the kinetic energy of the flow and causes a transition from super- to subcritical flow behaviour. We discuss this feature in terms of the possible effectivity of snow nets as avalanche catching structures.

2 EXPERIMENTAL SETUP

The setup of the laboratory chute is shown in Figure 1.

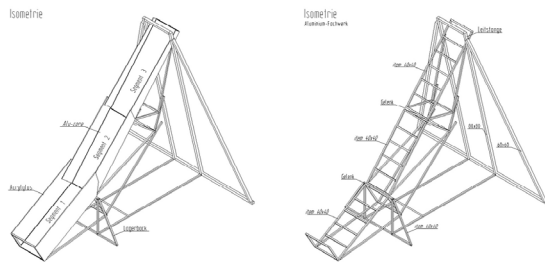


Figure 1: 3 Dimensional view of the chute

2.1 Chute geometry

The chute consists of three sections. The inclination of each of the about 2.5 m long sections of the chute can individually be varied so that the chute can model gross features of an avalanche track such as release area, avalanche track and run-out zone.

2.2 Instrumentation

For the measurement of velocity, we used digital video cameras and optical velocity sensors. Four cameras with a frame rate of 60 fps were mounted at the chute to record side views (three cameras) and front views (one camera) of the model avalanches. Velocities were estimated by analysing the frames with regard to grids on the ground and on the sidewalls.

Furthermore, we used a high-speed camera to take side views of the model avalanches with a frame rate 480fps. This high time resolution allows to estimate the quasi-instantaneous velocity distribution in the avalanche body and head (see fig. 5) with Particle Image Velocimetry (PIV).

At the downhill end of the second chute section (see fig. 1), two optical velocity sensors were installed to record the basal velocity along the avalanche.

2.3 Materials for avalanche simulation

To study the influences of material properties on the evolution of model avalanches and, in particular, to explore a wide range of density ratios, we tested three different materials: lime wood (LH), glass foam (GS) and polystyrol (PS). The polystyrol particles had been specially manufactured. They consist of PS and graphite to minimise electrostatic effects. The properties of the materials used in the experiments such as the particle diameter D , the particle and bulk densities ρ_p and ρ_b are shown in Table 1.

material	D mm	ρ_p kg/m ³	ρ_b kg/m ³
lime wood	4	450	320
glass foam	1-4	330	210
PS heavy	2-4	271	186
PS medium	3-4	171	118
PS light	4	71	50

Table 1: Properties of model materials

3 RESULTS

3.1 Avalanche experiments

From Figure 2, we observe that the flow velocities and the height of the avalanche heads increase with the chute inclinations. The head height also depends on which material is used in the experiment (different elasticities). The front of the “GS avalanche exhibits a front instability also called “fingering (see fig.3). Regarding the PS avalanches, this effect gets even stronger: the front of the PS avalanches (fig. 4) are getting to split up in two or more rotational heads.

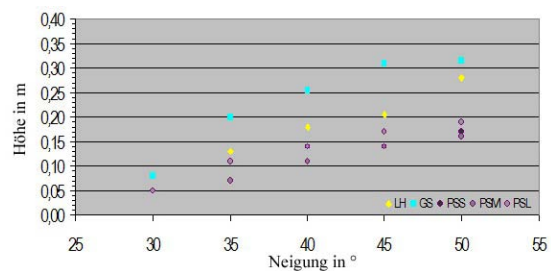


Figure 2: Dependency of front heights from chute inclination

The results of the PIV analysis of the high-speed camera recordings of the avalanche front show a decrease of velocity with height which indicates the presence of a rotational head such as described by McElwaine and Turnbull (2005).



Figure 3: Fingering at the front of a GS avalanche

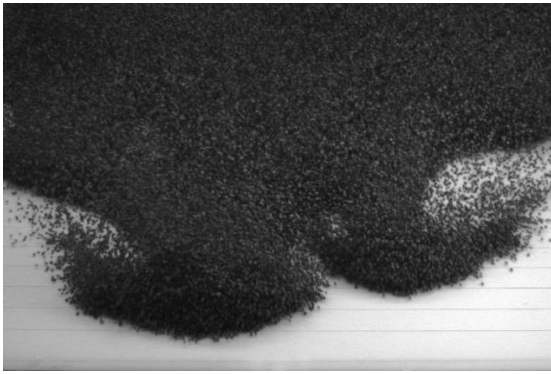


Figure 4: PS avalanche with two rotational heads

3.2 Snowcatcher experiments

To judge the effectivity of snow nets as avalanche catching structures, a scaled model of a so-called "snowcatcher structure was placed in the run-out zone of the chute. A PIV velocity field analysis was performed on high-speed camera takes of the particle passage through the net and the jump of a part of the flow over the obstacle. As a striking feature, the velocity plots show approximately constant velocities after the flow has passed the snowcatcher, independently of the flow properties before.

4 ANALYSIS

To characterize the model experiments, we use dimensionless numbers. To calculate the Froude-, Reynolds- and Stokes-numbers, velocity, density, flow height and particle diameter are taken into account. We estimate the velocity from video camera frames and by optical velocity sensors. Estimating the mean density of the fluidised/suspended part of the model

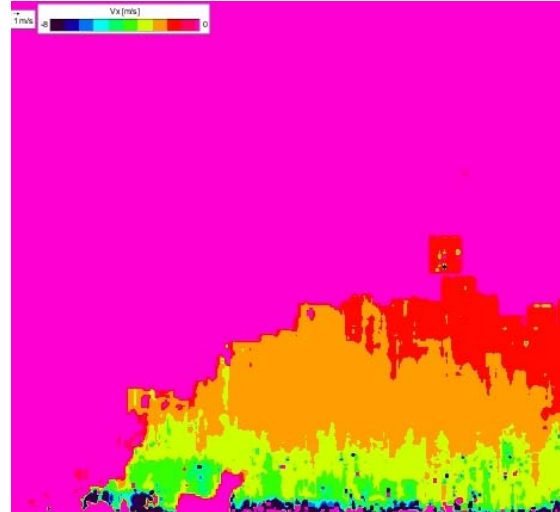


Figure 5: Velocity distribution in the avalanche head

avalanches is the most difficult challenge. To get a rough estimate, we count the particles in the fluidised suspension layer. This method allows to state boundaries upon the density of the fluidised flow parts.

Referring to the notation in Figure 7, we are able to estimate the energy dissipation of an avalanche due to the impact on the snowcatcher. Kinetic and potential energy are calculated at defined points 1 and 2 using Equations (1) – (3):

$$e_0 = \frac{v_0^2}{2} + g \cdot \frac{h_0}{2} \cdot \cos \alpha \quad (1)$$

$$e_1 = \frac{v_1^2}{2} + g \cdot \left(L_{SN} \cdot \sin(\beta - \alpha) + \frac{h_1}{2} \cdot \cos(\beta - \alpha) \right) \quad (2)$$

$$e_2 = \frac{v_2^2}{2} + g \cdot \left(L_{SN} \cdot \sin(\beta - \alpha) - \frac{h_2}{2} \cdot \cos \alpha \right) \quad (3)$$

Equation 4 gives an approximation of energy dissipation.

$$E_{diss} = \frac{e_1 + e_2}{e_0} \cdot 100 \quad (4)$$

The results indicate that approximately 2/3 of the kinetic energy are dissipated at the snowcatcher.

5 DISCUSSION

We now shortly indicate some advantages and disadvantages of scaled avalanche experiments that use air as ambient medium. Table 2 shows the Froude number (plain and densimetric) and the density ratio $\Delta\rho/\rho_a$. A comparison with natural avalanches shows that the ranges of these dimensionless measures match quite satisfyingly.

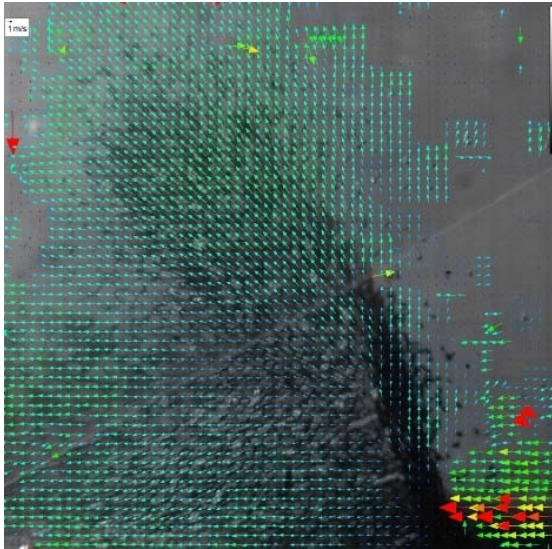


Figure 6: Vector plot of avalanche impact in the snowcatcher

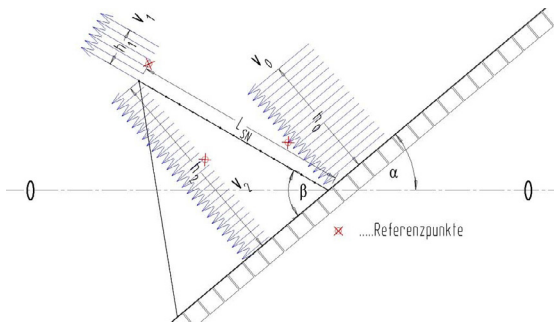


Figure 7: Model of avalanche impact

	Fr	Fr _d	$\Delta\rho/\rho_a$
PSS	6,5 – 7,3	1,0 – 2,3	10,3 – 44,0
PSM	6,1 – 7,2	1,2 – 2,9	6,1 – 27,3
PSL	5,3 – 6,3	1,4 – 2,4	2,0 – 10,9
GS	4,7 – 6,8	0,6 – 1,9	12,8 – 54,0
LH	3,3 – 5,4	0,4 – 1,3	17,8 – 74,0
NA	2 – 15	0,7 – 2,7	10 – 40

Table 2: Froude- and densimetric Froude number, density ratio. PSS: heavy polystyrol particles, PSM: medium weight polystyrol particles, PSL: light polystyrol particles, GS: glass foam particles, LH: lime wood speres, NA: natural avalanche

A comparison of the dimensionless numbers in Table 3 indicates lower turbulence levels in the experiments than in natural avalanches.

The high level of the Stokes-number in the experiments indicates a bad modelling of the suspension effect.

	Re	Re _p	St
PSS	$3,0 \cdot 10^5 - 6,0 \cdot 10^6$	594 – 1055	2,6 – 9,0
PSM	$1,8 \cdot 10^5 - 3,5 \cdot 10^6$	842 – 1516	2,7 – 8,5
PSL	$7,3 \cdot 10^4 - 1,6 \cdot 10^6$	993 – 1666	1,2 – 4,7
GS	$3,5 \cdot 10^5 - 3,8 \cdot 10^6$	707 – 1136	4,5 – 7,7
LH	$9,1 \cdot 10^5 - 1,3 \cdot 10^7$	942 – 2019	5,4 – 11,5
NA	$1,0 \cdot 10^9$	3000	0,02

Table 3: Reynolds-, Particle-Reynolds- and Stokes numbers. PSS: heavy polystyrol particles, PSM: medium weight polystyrol particles, PSL: light polystyrol particles, GS: glass foam particles, LH: lime wood speres, NA: natural avalanche

Calculating the Froude number before and after the impact on the snowcatcher, a transition from super- to (sub)critical flow behaviour can be observed (see tab. 4).

Exp	Inclination in °	before SC			after SC		
		v_0 m/s	h_0 cm	Fr_0 -	v_2 m/s	h_2 cm	Fr_2 -
PSL	20/30	3,6	3	6,63	0,9	9,6	0,91
	30/40	4,6	4	7,34	1,0	9,6	1,01
	35/45	5,4	5	7,71	1,1	9,6	1,11
	40/50	6,4	7	7,84	1,2	9,6	1,21
PSM	30/40	5,0	4	7,98	1,0	9,6	1,01
	35/45	5	10	7,58	1,1	9,6	1,11
	40/50	7	12	7,96	1,2	9,6	1,21

Table 4: Froude numbers **before** und **after** impact on snowcatcher. PSL: light polystyrol particles, PSM: medium weight polystyrol particles.

6 CONCLUSION

The wide range of densities of used model materials will allow to model a wide range of features of natural avalanches. Except the suspension of the particles in the surrounding air, the scaled model avalanches map the real-scale behaviour of avalanches quite well. A systematic in-deep analysis of the accessible values of the dimensionless quantities of the model avalanches will further clarify the practical use of scaled modelling for the design of protection structures against avalanches.

The snowcatcher experiments show that the flow is splitted into a penetrating and an overflowing part. Besides dissipation of $\sim 2/3$ of the kinetic energy, we observed a transition from super- to (sub)critical flow behaviour of the penetrating flow branch (that makes up the major mass of the flow).

In summary, we may state that the snowcatcher concept promises to be an economic way to protect settlements and infrastructure from avalanches.

To finally stop the (sub)critical flow behind the snow-catcher, further measures such as mounds or (low) retention walls are proposed.

ACKNOWLEDGMENTS

This work has been funded by FFG under grant No. 81544/12902 – SCK/KUG. Many thanks are due to the mechanical staff of BFW and IWB. Without their help, this work would not have been possible.

REFERENCES

- Hermann, J., F. Hermann and K. Hutter, 1986: Laboratory experiments on the dynamics of powder snow avalanches. *Proceedings of Avalanche Formation, Movements and Effects, IAHS publication*, Davos, volume 162, 431–440.
- McElwaine, J., 2005: Rotational flow in gravity current heads. *Phil. Trans. R. Soc. Lond. A*, **363**, 1603–1623.
- McElwaine, J. and B. Turnbull, 2005: Air pressure data from the Vallé de la Sionne avalanches from 2004. *J. Geophys. Res.*, **110**.
- Scheiwiller, T. and K. Hutter, 1982: Lawinendynamik: Uebersicht ueber Experimente und theoretische Modelle von Fliess- und Staublawinen. *Mitteilungen* 58, VAW.
- Turnbull, B. and J. McElwaine, 2008: Experiments on the non-boussinesq flow of self-igniting suspension currents on a steep open slope. *J. Geophys. Res.*, **113**, F01003.